Determining and benchmarking risk neutral distributions implied from option prices

Reference:

Salazar Celis Oliver, Liang Lingzhi, Lemmens Damiaan, Tempère Jacques, Cuyt Annie A.M..- Determining and benchmarking risk neutral distributions implied from option prices

Applied mathematics and computation - ISSN 0096-3003 - 258(2015), p. 372-387

DOI: http://dx.doi.org/doi:10.1016/j.amc.2015.02.011

Determining and benchmarking risk neutral distributions implied from option prices☆

Oliver Salazar Celis[a,c,1,*], Lingzhi Liang[b], Damiaan Lemmens[b], Jacques Tempère[b,d], Annie Cuyt[a,**]

[a] *Computational Mathematics (CMA), University of Antwerp, Department of Mathematics and Computer Science, Middelheimlaan 1, 2020 Antwerpen, Belgium*
[b] *Theory of Quantum Systems and Complex Systems (TQC), University of Antwerp, Department of Physics, Universiteitsplein 1, 2610 Antwerpen, Belgium*
[c] *Avantage Reply, Congresstraat 5, 1000 Brussels, Belgium*
[d] *Lyman Laboratory of Physics, Harvard University, Cambridge MA02138, USA*

Abstract

Risk neutral probability density functions (RNDs) play a central role in assessing models for stock market behaviour. However, it remains challenging to distill a realistic estimate for the RND from empirical data. In this work we introduce a novel method to infer a RND estimate from observed option prices. Our method efficiently yields a realistic rational function approximation to the RND, it is flexible w.r.t. the shape of the underlying distribution and robust in the presence of noise. To show this, we first investigate how well a method can actually retrieve a known distribution from noisy option prices. Then we consider real market data and show how our method can be used to derive a single continuously differentiable RND estimate from empirical call and put option price data.

Keywords: Implied probability density function, Benchmarking, S&P 500 Index options, Rational approximations, Option pricing, Bid-Ask interval

1. Introduction

Stochastic models for option pricing implicitly assume an underlying risk neutral probability density function (RND). In order to calibrate these models as well as to identify limitations of these models, a comparison to the experimentally realized probability density function (PDF) is required. The most well-known example of such a comparison is the empirical observation that the tails of the reported return PDFs are fatter than expected under the Black-Scholes model [1]. This led to the development of improved models based on stochastic volatility, such as the Heston model [2], or jump-diffusion models [3, 4], or models based on Lévy processes [5, 6].

The main goal of the present paper is to introduce a new global and nonlinear approximation method to estimate the implied RND from option prices. Our new method is designed to tackle the two main problems that arise in determining option implied densities. These problems are (1) that there are only option prices for discrete sets of strikes, and (2) that these prices contain errors (e.g. due to the bid-ask spread, there is an 'error bar' on the price of any given option). Such errors can cause unrealistic density approximations. Our method attempts to overcome these drawbacks and yields a rational function approximation from interval data. Therefore we refer to our novel Rational Interval Interpolation method as the RII method.

Before the RII method is applied to real market data, we first compare it to some commonly used methods using simulated data with added noise. Only a small part of the literature [7, 8] uses simulated data to test the performance of methods to derive the implied RND. Nevertheless, we believe

[☆]This work was supported by the Research Foundation - Flanders (FWO), through research program nr. G.0125.08, and by the Special Research Fund of the University of Antwerp BOF NOI UA.

[*]Corresponding author

[**]Principal corresponding author. Tel. +32 (0)3 265 38 98, Fax +32 (0)3 265 37 77

Email addresses: oliver.salazarcelis@uantwerpen.be (Oliver Salazar Celis), lingzhi.liang@uantwerpen.be (Lingzhi Liang), damiaan.lemmens@uantwerpen.be (Damiaan Lemmens), jacques.tempere@uantwerpen.be (Jacques Tempère), annie.cuyt@uantwerpen.be (Annie Cuyt)

[1]The information and the views set out in this article are those of the author and do not necessarily reflect the official opinion of Avantage Reply. Avantage Reply does not guarantee the accuracy of the data included in this article. Neither Avantage Reply, nor any person acting on its behalf may be held responsible for the use which may be made of the information contained therein.

that simulated data from a known underlying PDF guarantees a fair comparison of the methods in a controlled environment. After confirming that our method yields reliable results, we then look at real data and estimate RNDs from S&P 500 index options. It is shown how our method is used in practice: how to deal with no-arbitrage considerations and exploit the availability of put prices.

The paper is structured as follows. In Section 2 we detail on some selected methods to estimate a RND from option price data. In Section 3 we present the details of our novel RII method to estimate a RND. In Section 4 we discuss how simulated data are generated and we present our benchmark, we compare and discuss the performances of the aforementioned approaches. Section 5 is devoted to the application of our RII method to real market data. And finally, a conclusion is drawn in Section 6.

2. Selected methods

There exist a variety of approaches for extracting the RND in the literature that can be followed. For instance, in the Maxent method [9] and subsequent developments [10, 11, 12, 13], the asset distributions are obtained by maximizing an entropy representing the information content. Maximizing the entropy corresponds to minimizing the amount of uncontrolled assumptions in the derivation [14, 15]. It can be shown [16] that using Shannon's entropy (or, equivalently, minimizing the Kullback-Leibler distance) leads to distributions within the exponential family. Hence, in these approaches, the choice of distribution family is linked to the choice of entropy function, whereas in our approach we want to include the possibility of non-exponential distributions. Without the intend to be exhaustive, we refer to [17, 18, 19, 20, 21, 22, 23, 8, 24] for other possible methods to infer the implied RND.

Methods for extracting an estimate for the RND from option prices basically rely on the following. Suppose that at a certain time $t = T$ the asset price S_T has a conditional RND $P(S_T, T|S_0)$, where the condition stipulates the initial value S_0 of the asset at time $t = 0$. Since the payoff of a plain vanilla European call option with strike K and maturity T is $\max[S_T - K, 0]$, the price C of this call option can be calculated as

$$C(S_0, K, T) = e^{-rT} \int_K^\infty (S_T - K) P(S_T, T|S_0) dS_T, \tag{1}$$

where e^{-rT} is a discount factor with interest rate r. Differentiating this formula twice with respect to K we get

$$\left.\frac{\partial^2 C(S_0,K,T)}{\partial K^2}\right|_{K=S_T} = e^{-rT}\frac{\partial}{\partial K}\left(-\int_K^\infty P(S_T,T|S_0)dS_T\right)\Bigg|_{K=S_T}$$
$$= e^{-rT}P(S_T,T|S_0) \quad .$$

Note that the PDF is normalized, hence we get

$$\int_{-\infty}^{\infty}\left.\frac{\partial^2 C(S_0,K,T)}{\partial K^2}\right|_{K=S_T} dK = e^{-rT}.$$

The implied RNDs is then straightforwardly given by [25]

$$P(S_T,T|S_0) = e^{rT}\left.\frac{\partial^2 C(S_0,K,T)}{\partial K^2}\right|_{K=S_T}. \tag{2}$$

As already mentioned there are some problems to bring this theoretical relation into practice, such as the fact that only a discrete set of strikes is available. Also, the market mechanism of bidding and asking results in a "measurement error" or uncertainty on the observed option prices, through the bid-ask spread.

2.1. Implied volatility surface (IVS) approach

A popular approach to cope with these problems is the one based on smoothing the volatility smile like in [26, 27, 28]. For this method, option prices are first transformed to a certain volatility curve. In a Black-Scholes setting with risk neutral interest rate r and volatility σ, the European vanilla call option price is given by:

$$C = S_0 N(d_+) - Ke^{-rT}N(d_-), \tag{3}$$

where $N(.)$ is the standard normal cumulative distribution function, and

$$d_\pm = \frac{1}{\sigma\sqrt{T}}\ln\left(\frac{S_0}{K} + \left(r \pm \frac{\sigma^2}{2}\right)T\right). \tag{4}$$

Expressions (3) and (4) can be used to convert the option prices $C(S_0, K, T)$ into an implied volatility surface $\sigma(S_0, K, T)$. Next, this implied volatility surface is smoothed with a cubic spline, and the smoothed surface is mapped back onto a smoothed option price function. This smoothed option price function allows for taking a second derivative and determining the (discounted) RND through expression (2).

2.2. Double lognormal (DLN) approach

Another commonly used approach is the DLN approach [29, 7, 30, 31]. In this framework, one assumes that the RND of S_T is given by a double lognormal distribution:

$$P(S_T) = \frac{b}{S_T\sigma_1\sqrt{2\pi T}} \exp\left\{-\frac{1}{2\sigma_1^2 T}\left[\ln\left(S_T/S_0\right) - \left(m_1 - \frac{\sigma_1^2}{2}\right)T\right]\right\} + \frac{1-b}{S_T\sigma_2\sqrt{2\pi T}} \exp\left\{-\frac{1}{2\sigma_2^2 T}\left[\ln\left(S_T/S_0\right) - \left(m_2 - \frac{\sigma_2^2}{2}\right)T\right]\right\}.$$

In this expression, the fitting parameters m_1, m_2 are drifts, σ_1, σ_2 are volatilities and b determines the relative contribution of the two lognormal densities. The price of a European vanilla call option is then given by

$$\begin{aligned} C &= be^{-rT}\left[e^{m_1 T}S_0 N(d_+^{(1)}) - KN(d_-^{(2)})\right] \\ &\quad + (1-b)\,e^{-rT}\left[e^{m_1 T}S_0 N(d_+^{(1)}) - KN(d_-^{(2)})\right], \end{aligned} \tag{5}$$

with

$$d_\pm^{(j)} = \frac{1}{\sigma_j\sqrt{T}}\ln\left(\frac{S_0}{K} + \left(m_j \pm \frac{\sigma_j^2}{2}\right)T\right).$$

The parameters $m_1, m_2, \sigma_1, \sigma_2, b$ and r in (5) are determined by minimizing the least squares distance to the observed market prices. Since this method requires six nonlinear parameters to be determined, it can easily strand in a local minimum and thus is prone to yield unreliable results.

3. Rational interval interpolation (RII) approach

For an in-depth discussion about the approximation properties of rational functions we refer to [32, p.187 §§ 23-28], [33] and the references therein. In the current context, the basic problem statement of RII starts from the

following. Instead of an observed option price point value $\tilde{C}_i$, it is assumed that an interval $[\underline{c}_i, \overline{c}_i]$ is given at each (distinct) strike K_i $(i = 0, \ldots, n)$. In practice the bounds $\underline{c}_i < \overline{c}_i$ are in a natural way obtained from the market mechanism of bidding and asking, as illustrated in Section 5.

We then look for an irreducible rational function $r_{\ell,m}(K) = p_\ell(K)/q_m(K)$ consisting of a numerator polynomial $p_\ell(K)$ of degree at most ℓ and a denominator polynomial $q_m(K)$ of degree at most m, with $\ell + m \ll n$ and such that the interval interpolation conditions

$$r_{\ell,m}(K_i) \in [\underline{c}_i, \overline{c}_i] \quad \Leftrightarrow \quad \underline{c}_i \leq r_{\ell,m}(K_i) \leq \overline{c}_i, \qquad i = 0, \ldots, n \tag{6}$$

are satisfied. Provided that $q_m(K_i) > 0$, it is detailed in [34] that the coefficients of $r_{\ell,m}(K)$ have to satisfy the linear inequalities

$$\begin{cases} -\overline{c}_i q_m(K_i) + p_\ell(K_i) \leq 0 \\ \underline{c}_i q_m(K_i) - p_\ell(K_i) \leq 0 \end{cases}, \qquad i = 0, \ldots, n. \tag{7}$$

Note that the rational interval interpolant $r_{\ell,m}(K)$ carries a double index to indicate the numerator and denominator degree. Although it may be preferable to carry this double index over to the numerator and denominator polynomial, we prefer to write $r_{\ell,m}(K) = p_\ell(K)/q_m(K)$. This is more convenient in the sequel (see Appendix B) when we compute two rational interval interpolants interpolating in different regions but sharing a common denominator. The context in which the rational interval interpolants are used ensures that our notation does not become ambiguous.

Our goal is not merely to approximate option prices, but also to derive an approximation from it for the (discounted) RND using the relation (2), i.e. by differentiating an approximation $r_{\ell,m}(K)$ for the option price twice w.r.t. K. One of the advantages of using a rational approximation $r_{\ell,m}(K)$ is the fact that it is infinitely differentiable and its second derivative can easily be written down explicitly. However, by definition, derivatives are quite sensitive to small oscillations of the underlying function. Artificial oscillations typically appear in approximations constructed from data subject to (heavy) noise. This may result in inaccurate and unrealistic density approximations. Fortunately, the theoretical prices of European vanilla call options are known to be convex decreasing functions of K. Hence, in order to guide the approximations towards more realistic shapes, we add the following (discrete) conditions for the first and the second derivative.

The theoretical price of a European vanilla call option is monotonically decreasing with respect to the strike K and the value of its derivative is bounded between $-e^{-rT}$ and 0. It is known that [25]

$$\frac{\partial C}{\partial K}(K) = -e^{-rT}\left(1 - \mathrm{CDF}(K)\right),$$

where $\mathrm{CDF}(K)$ is the cumulative distribution function corresponding to the underlying PDF. Therefore we add the conditions at the locations K_i that

$$-e^{-rT} \leq r'_{\ell,m}(K_i) = \frac{p'_\ell(K_i) - r_{\ell,m}(K_i)\, q'_m(Ki)}{q_m(K_i)} \leq 0, \qquad i = 0, \ldots, n. \quad (8)$$

Here $r'_{\ell,m}(K)$ denotes the first derivative of $r_{\ell,m}(K)$ w.r.t. K. Provided that both $q_m(K_i) > 0$ and (6) are satisfied, (8) is also satisfied if

$$\begin{cases} p'_\ell(K_i) - \overline{c_i}\, q'_m(K_i) \leq 0 \\ p'_\ell(K_i) - \underline{c_i}\, q'_m(K_i) \leq 0 \\ -e^{-rT} q_m(K_i) - p'_\ell(K_i) + \overline{c_i}\, q'_m(K_i) \leq 0 \\ -e^{-rT} q_m(K_i) - p'_\ell(K_i) + \underline{c_i}\, q'_m(K_i) \leq 0 \end{cases}, \quad i = 0, \ldots, n. \quad (9)$$

Second, because a CDF is monotonically increasing w.r.t. its random variable, the first (partial) derivative of the theoretical European vanilla call option price is also monotonically increasing with respect to K. Therefore we also add the discrete conditions for $i = 0, \ldots, n$

$$0 \leq r''_{\ell,m}(K_i) = \frac{p''_\ell(K_i) - r_{\ell,m}(K_i)\, q''_m(K_i) - 2\, r'_{\ell,m}(K_i)\, q'_m(K_i)}{q_m(K_i)}. \quad (10)$$

Provided that (6), (8) and $q_m(K_i) > 0$ hold, (10) is satisfied if

$$\begin{cases} -p''_\ell(K_i) + \overline{c_i}\, q''_m(K_i) - 2\, e^{-rT}\, q'_m(K_i) \leq 0 \\ -p''_\ell(K_i) + \overline{c_i}\, q''_m(K_i) \leq 0 \\ -p''_\ell(K_i) + \underline{c_i}\, q''_m(K_i) - 2\, e^{-rT}\, q'_m(K_i) \leq 0 \\ -p''_\ell(K_i) + \underline{c_i}\, q''_m(K_i) \leq 0 \end{cases}, \quad i = 0, \ldots, n. \quad (11)$$

Although the conditions (8) and (10) are merely imposed on a discrete set and therefore do not prevent violations in between given strikes, they seem to work very well in practice [35]. Moreover, it can be shown that when discrete conditions are imposed at sufficiently many locations, the condition is

implied in between all locations [36]. Unfortunately, the theoretical number of discrete conditions needed for this implication to hold is often too high to be of practical use. Guaranteeing a rational approximation with a nonnegativity second derivative on the entire real line is currently out of scope here, but the interested reader is referred to [37].

For fixed ℓ and m, the problem that remains, is to obtain nonzero values for the coefficients of $r_{\ell,m}(K)$ such that the homogeneous linear inequalities (7), (9) and (11) are satisfied. We propose the computation of a Chebyshev direction [34], which essentially requires solving a strictly convex quadratic programming (QP) problem. Further details are given in Appendix B. To improve the numerical conditioning of the optimization problem, it is advised to rescale the given strikes K_i to the interval $[-1, 1]$ and to use orthogonal polynomials (e.g. Chebyshev polynomials) as basis functions rather than the monomials.

Concerning the values of ℓ and m, we remark the following. The total model complexity is determined by the total number of coefficients, i.e. $\ell + m + 2$. A low model complexity is desired to avoid overfitting effects such as artificial oscillations occurring due to modelling noise rather than (price) information. However, for a priori fixed ℓ and m, the QP problem may not have a solution when the required accuracy and derivative conditions cannot be met with the current choice for ℓ and m. In search for a feasible solution, the values of ℓ and m can first be varied by keeping $\ell + m$ constant. The sum $\ell + m$ is increased slowly but steadily until a solution is found. To reduce the overwhelming choice for the degrees ℓ and m, we can restrict ourselves in practice to the diagonal interpolants $r_{m,m}(K)$ and the para-diagonal $r_{m+1,m}(K)$ and $r_{m-1,m}(K)$. These three types of rational interpolants model all types of asymptotic behaviour. In Section 4 our focus is mainly on the center of the distribution. To maintain comparable results among the different settings, we fix the possible values for ℓ and m to those where $\ell = m + 1$. With this choice the rational function can exhibit an oblique as well as an almost horizontal asymptote (with a very small leading numerator coefficient). Hence, in Section 4 we only consider $\ell = m + 1$ and for increasing values of $m = 0, 1, 2, \ldots$ we solve a QP problem until a feasible solution is found. As an example, when using the aforementioned solver it takes about half a second (0.5 sec) on a standard desktop computer for MATLAB to enumerate over increasing $m = 0, 1, 2, \ldots$ and determine the existence and the coefficients of the rational function with $\ell = 21$ and $m = 20$ shown in Figure 5. We reconsider the choice for ℓ and m in the more

realistic case of Section 5, when the tails of the distribution can be modelled more accurately using both call and put prices.

4. Benchmark

4.1. Simulated data and market models

A large part of the literature (for a typical example, see [17]) uses market data to test the performance of methods for option implied densities. In [18], the robustness of the DLN and IVS methods is investigated by comparing the obtained implied densities from real option prices to those obtained by adding a small error to these market prices. Rather than using market data directly, with an essentially still uncertain RND, we use simulated data based on known RNDs first, and then add noise. This allows us to accurately test and benchmark the different approaches to imply a probability density function from noisy data.

Three different models of the market are considered in this paper. The first model to simulate market data is of course the Black-Scholes model [1], characterized by the following stochastic differential equation for the asset price $dS = \mu S dt + \sigma S dW$, where dW is a Gaussian process, and where we choose as a drift $\mu = 0.05$, volatility $\sigma = 0.2$, a risk neutral interest rate $r = 0.03$ and the value $S_0 = 925$. The same parameter values for r, μ and S_0 are used for the next two models.

The second model, also not a surprise, is the Heston model [2], characterized by two coupled stochastic differential equations

$$\begin{cases} dS = \mu S dt + \sqrt{v} S dW_1 \\ dv = \kappa(\theta - \nu)dt + \sigma_v \sqrt{v} dW_2 \end{cases},$$

with dW_1 and dW_2 two Gaussian processes. The parameters for the Heston model are chosen so that the resulting distribution lies close to a lognormal distribution: the mean reversion rate is $\kappa = 2$, the mean reversion level is $\theta = 0.04$ and the volatility is $\sigma_v = 0.1$. The correlation $\rho = \langle dW_1 dW_2 \rangle$ is chosen to be $\rho = 0.5$, and the variance at inception (at time $t = 0$) is set to $v_0 = 0.0437$. This model allows to check whether a small deviation from the lognormal model already influences the performance of the methods.

The third model belongs to a class of models known as Lévy models [5], where the increments of the logreturn $X_T = \ln(S_T/S_0)$ are drawn from a Lévy distribution. We choose the CGMY model [38], where the characteristic

function $\phi(\omega)$ associated with the distribution of the increments dX can be written as $\phi(\omega) = \exp[f(\omega)dt]$ with the characteristic exponent [39]

$$f(\omega) = C\,\Gamma(-Y)\left[(M - i\omega)^Y + (G + i\omega)^Y - G^Y - M^Y\right],$$

where C, G, M, Y are the parameters giving this model its name, and $\Gamma(\cdot)$ is the Euler gamma function. In the mean-correcting martingale measure [5], a new characteristic exponent $\hat{f}(\omega) = f(\omega) + i\omega\,(r - f(-i))$ is used, such that the asset price discounted by the bank account is a martingale

$$\mathbb{E}\left[\frac{S_T}{e^{rT}}\right] = S_0\,e^{-rT}\mathbb{E}\left[e^{x_T}\right] = S_0\,e^{\hat{f}(-i)T - rT} = S_0.$$

We choose parameter values $C = 0.0244$, $G = 0.0765$, $M = 7.5515$, $Y = 1.2945$. The corresponding distribution differs substantially from the lognormal distribution as illustrated in Figure 1. Nevertheless the parameter values for this model are realistic since they are obtained by calibrating a set of European call options on the S&P500 index [5].

We first analytically generate option prices [40, 41, 42, 43] for various strikes K_i. In total 56 distinct strikes are chosen at equidistant locations in the interval (including the endpoints) with mid-point equal to the forward value $F = S_0 e^{rT}$ and radius equal to 4 times the standard deviation of the underlying PDF. At a single maturity time, such a number of strikes is typical. Illustrations of the associated denstities following this setup are shown in Figure 1.

Then noise is added to the corresponding exact option prices C_i and we apply the option implied density methods (DLN, IVS and RII) to see how well they perform in retrieving the original, known RND. This allows us to learn how different aspects of the market (Lévy nature, stochastic volatility, etc.) influence the performances of the aforementioned three methods. Moreover, we calculate the results for different time to maturities to see how the duration affects their performances as well.

The prices plus noise should be similar to market data. We construct the noise in such a way that it replicates the fact that the noise of financial data is smallest around the forward value F and largest in the tails. Here $F = S_0 e^{rT}$ for all three above mentioned models and the values $T = 0.0384$, $T = 0.5$ and $T = 1.5$ (year) are chosen. Hence $F = 926.78$, $F = 948.42$ and $F = 997.04$ respectively. To determine where the tails start we use the

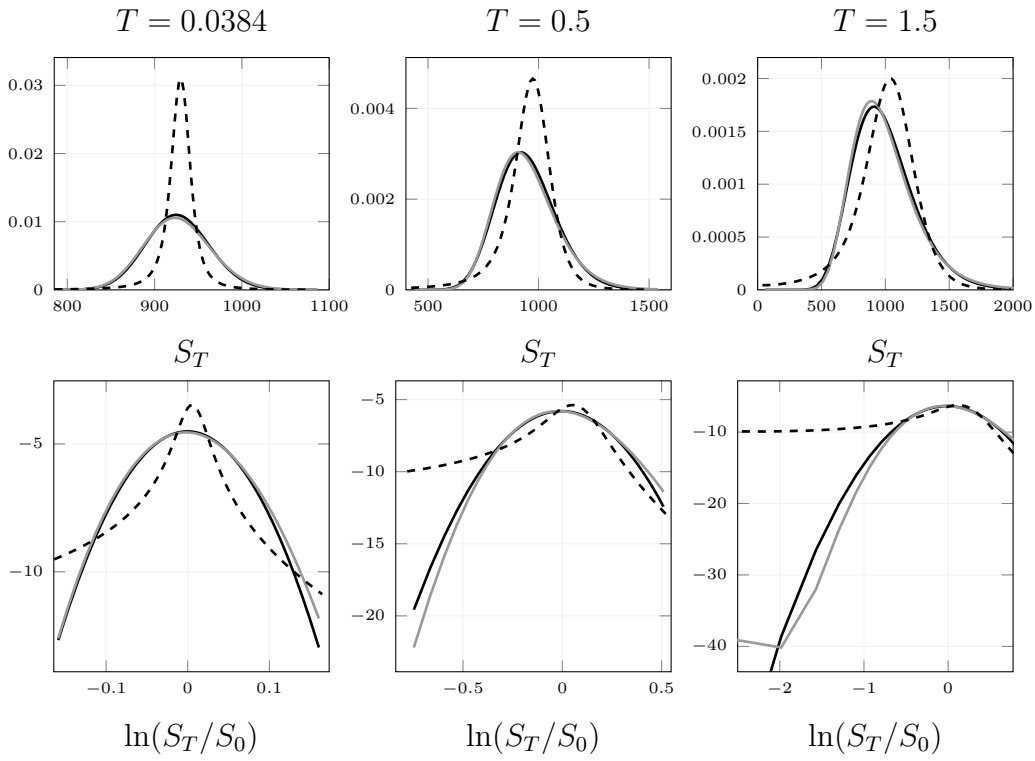

Figure 1: Illustration of the different distributions (top panels) used to test the DLN, the IVS and the RII method. From left to right, time ranges from 0.0384 to 0.5 to 1.5 year. The full black curve represents the lognormal distribution , the gray line the Heston distribution and the black dashed line the CGMY distribution. The bottom panels illustrate the lognormal nature of each of the distributions. The logarithm of the distributions is shown in function of the logreturns $\ln(S_T/S_0)$. As envisioned, the Heston distribution closely resembles the parabola of the lognormal distributions; whereas the CGMY distributions deviates substantially from it.

standard deviation s. For each option price a relative error is chosen from a uniform distribution on an interval $[-\beta, \beta]$ where β is determined by

$$\beta(K) = \eta \left(0.00025 \frac{|F - K|}{s} + 0.0001 \right). \tag{12}$$

Figure 2 illustrates the typical behavior of the relative errors for chosen values of the control parameter η equal to 1, 10 and 100 respectively.

For the RII method, intervals $[\underline{c}_i, \overline{c}_i] = [C_i(1 - \delta_i), C_i(1 + \epsilon_i)]$ are constructed for each of the strikes K_i $(i = 0, \ldots, 55)$. Like before, C_i denotes

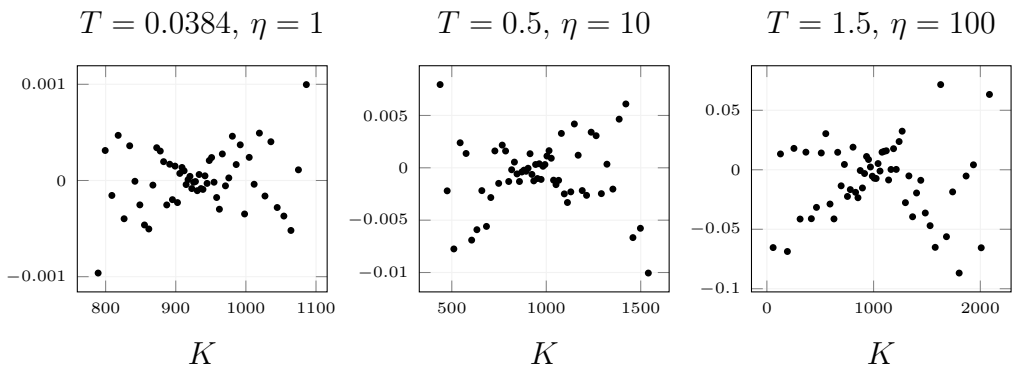

Figure 2: This figure represents a sample set of the relative errors for different values of η (and time to maturity T in years). In the left panel $\eta = 1$ (and $T = 0.0384$), in the middle one $\eta = 10$ (and $T = 0.5$), and in the right one $\eta = 100$ (and $T = 1.5$). The relative errors increase as the value of η grows (independent of T).

the analytically obtained option price value at strike K_i. The relative errors $\epsilon_i = \delta_i > 0$ are chosen according to (12). Hence the widths of the intervals mimic the typical behavior of uncertainty in observed financial data: small for strikes close to the forward value and increasingly larger for strikes away from the forward value. Notice that in practice, bid and ask prices can be used directly to obtain $[\underline{c}_i, \overline{c}_i]$.

4.2. Results and discussion

The performance of the different methods is summarized in Table 1. In this table a method which renders a better implied distribution has more + signs, if the implied distribution is unacceptable a − is assigned to it. We discriminate between good and bad fits in the following way. Given N strikes K_i, let d_i denote the associated values of the exact distribution and d_i' the values of the approximated distribution, then we calculate a normalized average error ne as:

$$ne = \frac{1}{N \max(d_i)} \sum_i |d_i - d_i'| \,. \tag{13}$$

Absolute errors are used instead of relative errors because we want to concentrate on the center of the distribution. To compare the average errors of different PDFs, each average error is divided by the maximum value of the PDF. For example if $ne = 1$ then, on average, the absolute error in each point

is as large as the maximum value of the distribution, and the corresponding implied distribution is obviously worthless. If the implied distribution is zero in every data point then ne lies close to 0.5. When $ne \leq 0.1$ then the implied distribution starts to look like the original distribution. The obtained values ne are given in the appendix (Table A.4). Following the logic above and to facilitate the analysis below, we summarize these values as follows. We assign a $-$ sign when $ne > 0.1$. If $0.02 \leq ne \leq 0.1$ then a $+$ sign is assigned, when $0.004 \leq ne < 0.02$ a $++$ sign and when $ne < 0.004$ a $+++$ sign.

Table 1: Summary of the performances of the different methods to derive the implied RNDs. The double lognormal method is abbreviated by DLN, the method based on smoothing the volatility surface by IVS, and the method based on rational interval interpolation by RII. The results are presented for different times to maturity T and values of the noise control parameter η. We assign a $-$ sign when the average error ne as defined in (13) satisfies $ne > 0.1$. If $0.02 \leq ne \leq 0.1$ then a $+$ sign is assigned, when $0.004 \leq ne < 0.02$ a $++$ sign and when $ne < 0.004$ a $+++$ sign.

η	T	Black-Scholes			Heston			CGMY		
		DLN	IVS	RII	DLN	IVS	RII	DLN	IVS	RII
1	0.038	$++$	$++$	$+++$	$++$	$++$	$+++$	$+$	$++$	$+++$
	0.5	$-$	$++$	$+++$	$+$	$+$	$+++$	$-$	$++$	$+++$
	1.5	$-$	$++$	$+++$	$+$	$+$	$+++$	$-$	$-$	$+++$
10	0.038	$+++$	$+$	$++$	$+$	$+$	$++$	$+$	$+$	$++$
	0.5	$-$	$+$	$+++$	$+$	$-$	$+++$	$-$	$+$	$++$
	1.5	$+++$	$+$	$+++$	$+$	$-$	$+++$	$-$	$-$	$++$
100	0.038	$++$	$-$	$++$	$+$	$-$	$++$	$+$	$-$	$++$
	0.5	$+$	$-$	$++$	$+$	$-$	$++$	$+$	$-$	$++$
	1.5	$-$	$-$	$++$	$-$	$-$	$++$	$-$	$-$	$++$

Analyzing Figures 3, 4, 5 and Tables 1, A.3 and A.4 leads to the following conclusions regarding the three tested methods. First, it is apparent that only our newly introduced RII method delivers satisfactory RND approximations for each scenario. Second, the DLN method is unstable due to the six-dimensional nonlinear optimization problem involved (Table A.4). Although the RII method also yields a nonlinear function and in general has even more parameters, it does not suffer from such effects because the involved optimization is strictly convex. This makes the approach extremely tractable. Third, the DLN method, entirely as expected, is least flexible concerning the reproduction of RNDs differing substantially from the lognormal one. The IVS method on the other hand, seems to be flexible as far as it concerns handling data coming from models differing from the lognormal one. Nevertheless also for this method, the data can be from a model with a PDF

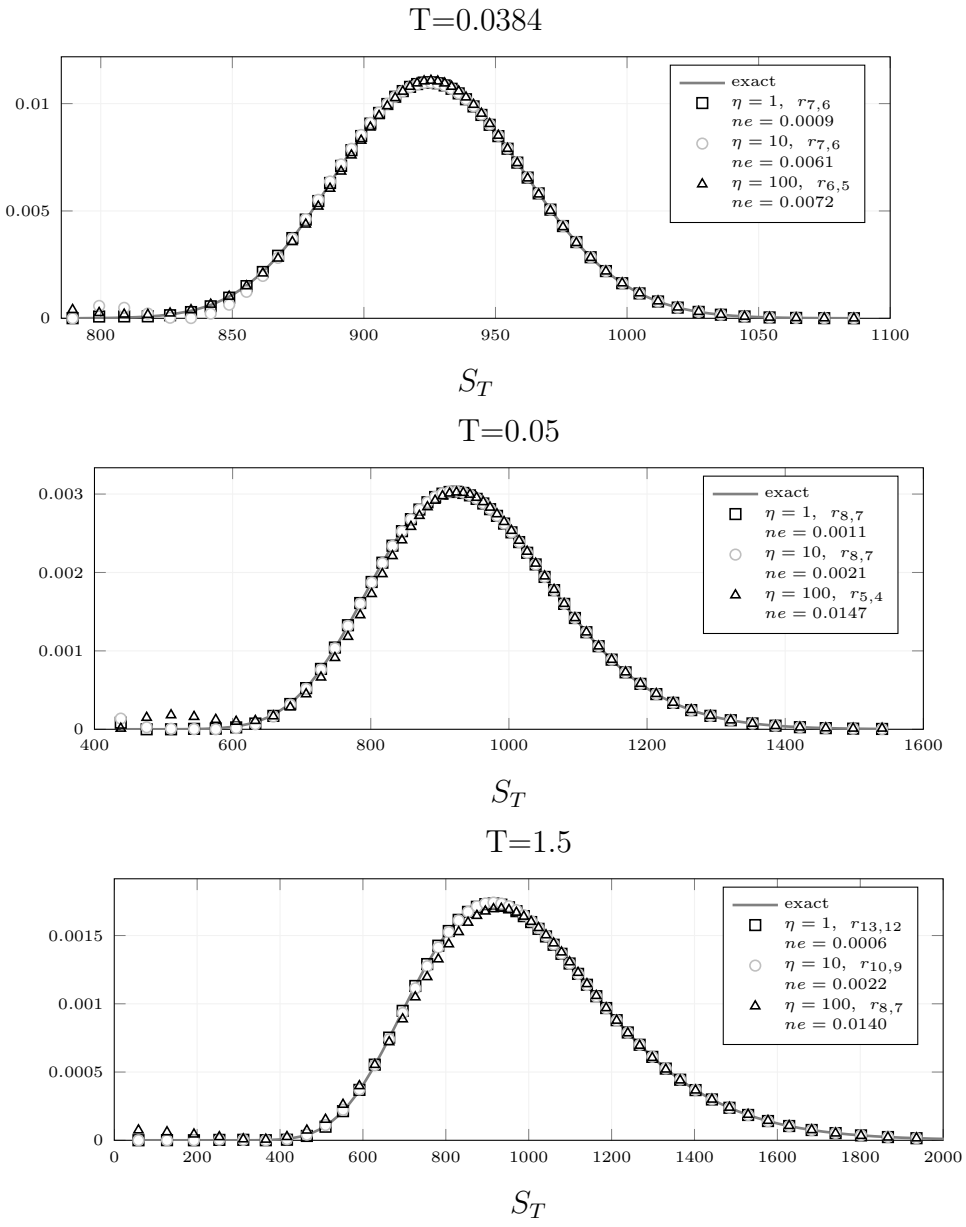

Figure 3: This figure illustrates the RII implied RNDs for the Black-Scholes data. From top to bottom, time T to maturity takes the value 0.0384, 0.5 and 1.5. In each panel, the full gray line is the exact PDF, while the squares, the circles and the triangles are the RII implied density approximations from the scenarios with control parameter $\eta = 1$, 10 and 100 respectively.

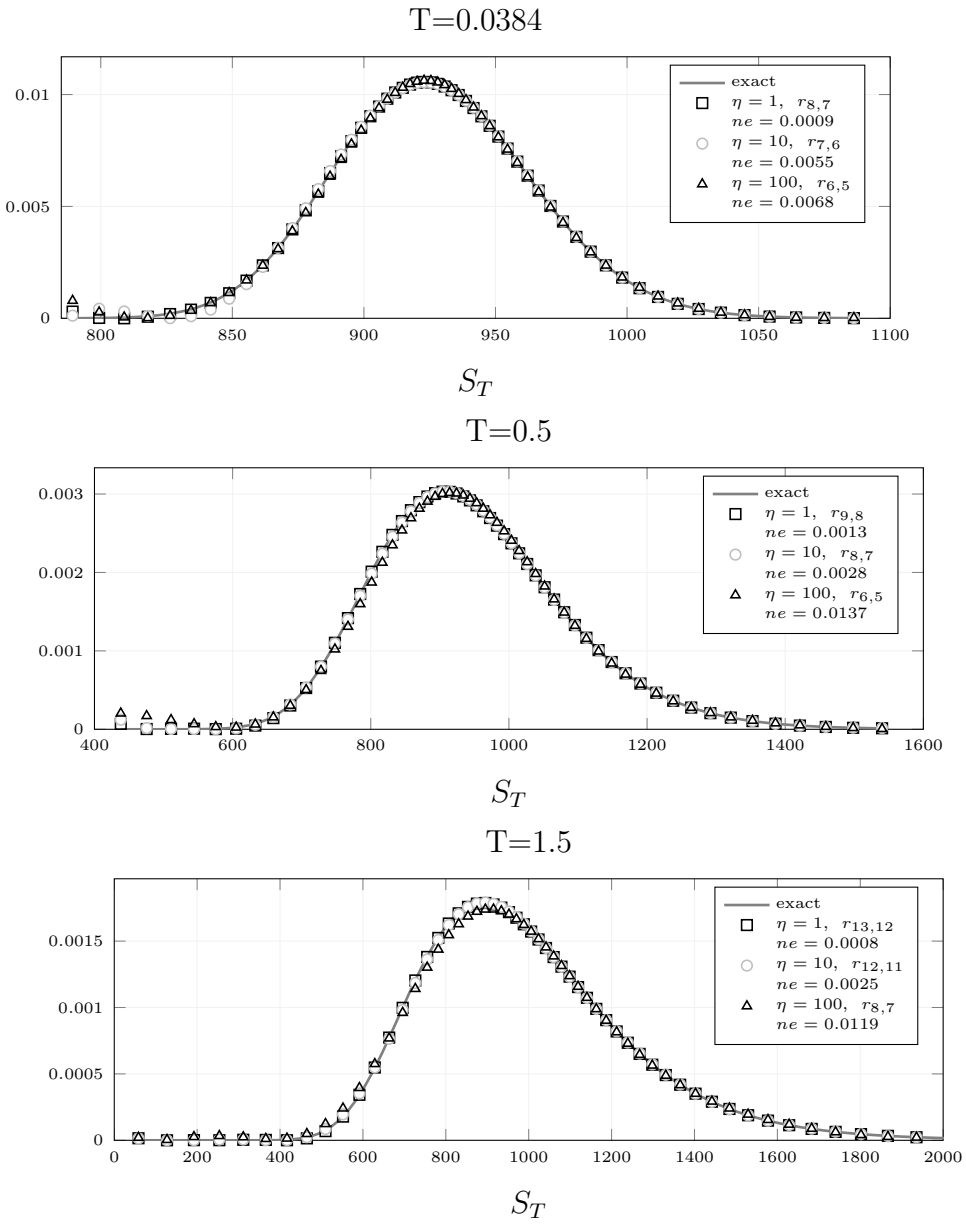

Figure 4: This figure illustrates the RII implied RNDs for the Heston data. From top to bottom, time T to maturity takes the value 0.0384, 0.5 and 1.5. In each panel, the full gray line is the exact PDF, while the squares, the circles and the triangles are the RII implied density approximations from the scenarios with control parameter $\eta = 1$, 10 and 100 respectively.

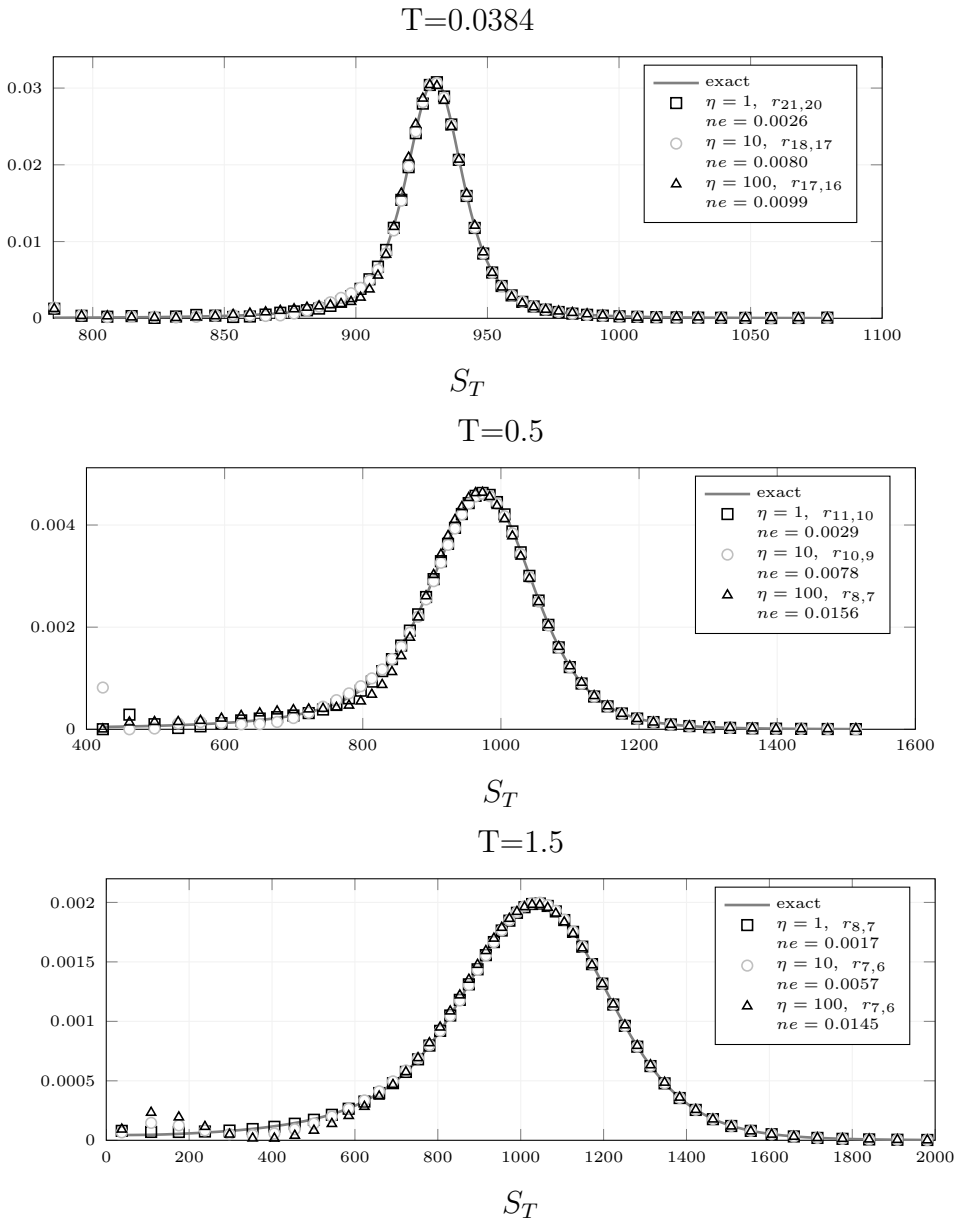

Figure 5: This figure illustrates the RII implied RNDs for the CGMY data. From top to bottom, time T to maturity takes the value 0.0384, 0.5 and 1.5. In each panel, the full gray line is the exact PDF, while the squares, the circles and the triangles are the RII implied density approximations from the scenarios with control parameter $\eta = 1$, 10 and 100 respectively.

which is too far from the lognormal one to be tractable. Fourth, it is seen that the IVS method is particularly sensitive to random errors, while the RII method is the most robust method in the presence of such errors.

Regarding the results of our RII method, we can say the following. First, for each market model and each time to maturity T, the deviation between the RII implied density and the original PDF understandably becomes larger as the value of the error control parameter η grows. Second, when keeping η and T fixed, the performance of the RII method typically decays with increasing skewness and kurtosis (Table A.3) of the underlying PDF. However, the final results are always satisfactory. Third, for each market model and each η, the values of the error criteria parameter ne are fairly similar for different time to maturities (Table A.4). Hence the maturity time T of the option hardly influences the performance of the method. Fourth, for each RII implied density, it is seen that the left tail approximation can be worse than the right tail approximation. It is worth noting that a similar phenomenon can be observed in the PDFs obtained in [24]. Here, this is mainly due to the fact that relative errors on large option prices (for small strikes) result in much larger absolute deviations than on small option prices (for large strikes). However, for small relative deviations (i.e. $\eta = 1$) the RII method is seen to deliver acceptable approximations.

The benchmark leads us to conclude that the commonly used DLN and IVS methods may lack reliability in a market that behaves more Heston-like or that has CGMY characteristics, and that the RII method is the most promising of the three considered techniques for implying RNDs from real option price data.

5. Application to market data

Now that it is demonstrated from simulated data that our RII implied density method produces reliable results, we are ready to apply the technique to real market data. We extract the implied RNDs from the daily closing bid and ask prices for Standard and Poor's 500 (S&P 500) Index options.

Unlike with simulated data, we now have no exact original density to benchmark, neither do we have the risk neutral interest rate r to discount the expected value to current time. By contrast, we have bid and ask prices from the market, which are quoted for all traded strikes no matter whether transactions occur or not. We use bid and ask prices directly to define the

interval data for our RII method and to measure the goodness of the estimated implied RND. If $[\underline{c}_i, \overline{c}_i]$ is the bid and ask interval at strike price K_i and ImpliedPrice(K_i) is the implied European vanilla option price derived from the (estimated) implied RND for that strike, then we define the relative position (RP) of this implied option price as:

$$RP(K_i) = \frac{\text{ImpliedPrice}(K_i) - \underline{c}_i}{\overline{c}_i - \underline{c}_i}. \tag{14}$$

If $RP(K_i)$ equals 0.5, then the implied price is exactly in the middle between bid and ask at strike price K_i. We call the implied density good if $RP(K_i)$ lies in between 0 (at the bid price) and 1 (at the ask price). The further the distance between the value $RP(K_i)$ and the interval $[0, 1]$, the worse the achieved implied RND.

Another difference between real data and the previously considered simulated data is the availability of put option prices. Analogous to the price of a European vanilla call option, the price of a European vanilla put option is given by the basic pricing formula

$$P(S_0, K, T) = e^{-rT} \int_0^K (K - S_T) P(S_T, T|S_0) dS_T. \tag{15}$$

Our RII method can be applied directly to derive an implied density from the put option prices after taking some straightforward modifications into account (which we omit due to space restrictions).

The goal of this section is to find a single implied RND and verify whether it reproduces feasible implied call and put option prices, i.e. the ImpliedPrice from the basic pricing formulas (1) and (15). A good implied RND reproduces implied option prices that are within the given bids and asks. We start with a detailed description of one example to explain the practical application of our RII method. Other examples, following the same reasoning, are given at the end of this section.

For data, we take the S&P 500 index call option prices as well as the put option prices of January 5th, 2005 with maturity time on March 18th, 2005 (72 days) [44, Table 1]. The S&P 500 index closing level is 1183.74, the interest rate is $r = 2.69\%$, and the dividend yield is $\delta = 1.7\%$. To determine the value of the discount factor e^{-rT}, we rely on the put-call parity

$$C(S_0, K, T) - P(S_0, K, T) = e^{-rT}(F - K), \tag{16}$$

where the forward price F is the expected price of S_T. The forward price F together with the discount factor e^{-rT} are obtained from a linear approximation of values $\tilde{C}_i - \tilde{P}_i$ as a function of common strike prices K_i. Here we obtain them from a best linear ℓ_1-norm approximation [45] using the midpoints of the given intervals as data values. Such an ℓ_1-approximation is least sensitive to outliers (for more details we refer to [46, Section 6.1]. The results of this approximation are shown in Figure 6 (right). We find $F = 1182.9$ and $e^{-rT} = 0.9948$. Since $T = 72/365$, we have the option traders' expected risk neutral return $r = 2.64\%$, which is a realistic value. Though the value F is slightly smaller than the index closing level 1183.74, it is still realistic due to the large uncertainty of that single last trade price.

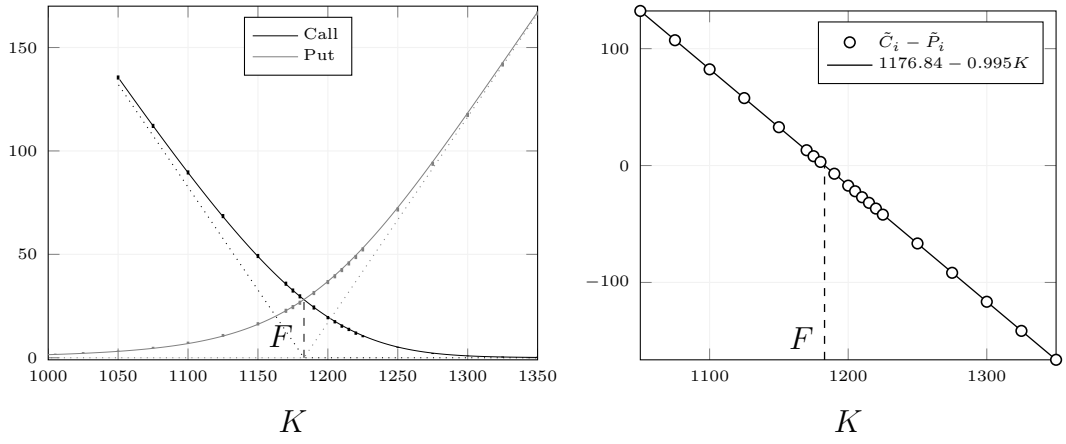

Figure 6: Left, the bid and ask call (black) and put (gray) price intervals from the S&P 500 index options of January 5th, 2005 with maturity date on March 18th, 2005. No-arbitrage lower bounds are shown with dots. Right, obtaining the forward value F and the discount factor e^{-rT} from the best linear ℓ_1-norm approximation of $C - P$, with circles the data and line the linear approximation. The vertical dashed line indicates the location of the forward price F.

Given the value of the discount factor above, we apply the RII method to both the call price interval data and the put price interval data. We obtain two rational approximations $r_{5,4}^{\text{call}}(K)$ and $r_{5,4}^{\text{put}}(K)$ shown in Figure 6 (left). Note that, in general, the obtained numerator and denominator degrees need not be the same for puts and calls. The two resulting implied densities are shown in Figure 7 (left). We find that these two implied RNDs differ too much to be reliable. Our goal is to obtain a single implied RND, suitable for both call price data and put price data.

For this purpose, first, we note that we can bring both curves r^{call} and r^{put} in better agreement by forcing the denominator polynomials to be the same, and the degrees of the numerator polynomials to be equal. The details of this procedure are outlined in Appendix B. Basically, the coefficients of both rational approximations are obtained from a single QP problem, which combines the QP problem of the RII method for call with the QP problem of the RII method for put into one. This is a simultaneous call-put RII method.

The idea behind the next step is that we use the call curve in the region where call prices are most reliable, and the put curve in the region where put prices are most reliable, and then glue the two curves together at an intermediate value: the forward price F, at which point the European vanilla call option price coincides with the European vanilla put option price. Put options are out-of-the-money when $K < F$, whereas for call options this is $K > F$. Then, we propose to use the implied density curve derived from $r^{\text{put}}(K)$ for $K < F$ and from $r^{\text{call}}(K)$ for $K > F$. This choice is supported by practice: the CBOE also calculates the VIX index by combining only out-of-the-money call and put contracts [47]. Moreover, we already obtain F from the determination of the discount factor. The results of this piecewise procedure with the basic RII method are shown in Figure 7 (top, left).

Subsequently, we ensure continuous differentiability at F, as explained in Appendix C, and obtain $r^{\text{call}}_{7,8}(K)$ and $r^{\text{put}}_{7,8}(K)$. The resulting (normalized) implied RND is shown in Figure 7 (top, right). The relative positions (14) are shown in Figure 7 (bottom). Almost all the implied prices are within their bid and ask intervals, from which we conclude with confidence that this RND reliably represents the single implied RND we are looking for.

A final important aspect is to guard against (static) arbitrage. In line with the reasoning of [20, 27, 48], we already imposed the shape constraints on the price approximations such as monotonicity, bound constraints on the first derivative and convexity/concavity (see (B.1)). However, no-arbitrage considerations also require the following conditions to be satisfied

$$\begin{cases} \max\left(0, e^{rT}K - e^{-\delta T}S_0\right) \leq C(S_0, K, T) \leq e^{-\delta T}S_0 \\ \max\left(0, e^{-\delta T}S_0 - e^{rT}K\right) \leq P(S_0, K, T) \leq e^{-\delta T}K \end{cases} . \tag{17}$$

We may discard the right-hand sides of (17), because they are generally less stringent than the upper bounds given by the bid-asks. However, the left-hand sides of (17), illustrated in Figure 6 by dotted lines, may tighten the bid-ask bounds for the put and call prices. In this example, the spot price $S_0 = 1180.8$ has been determined from the previously established forward

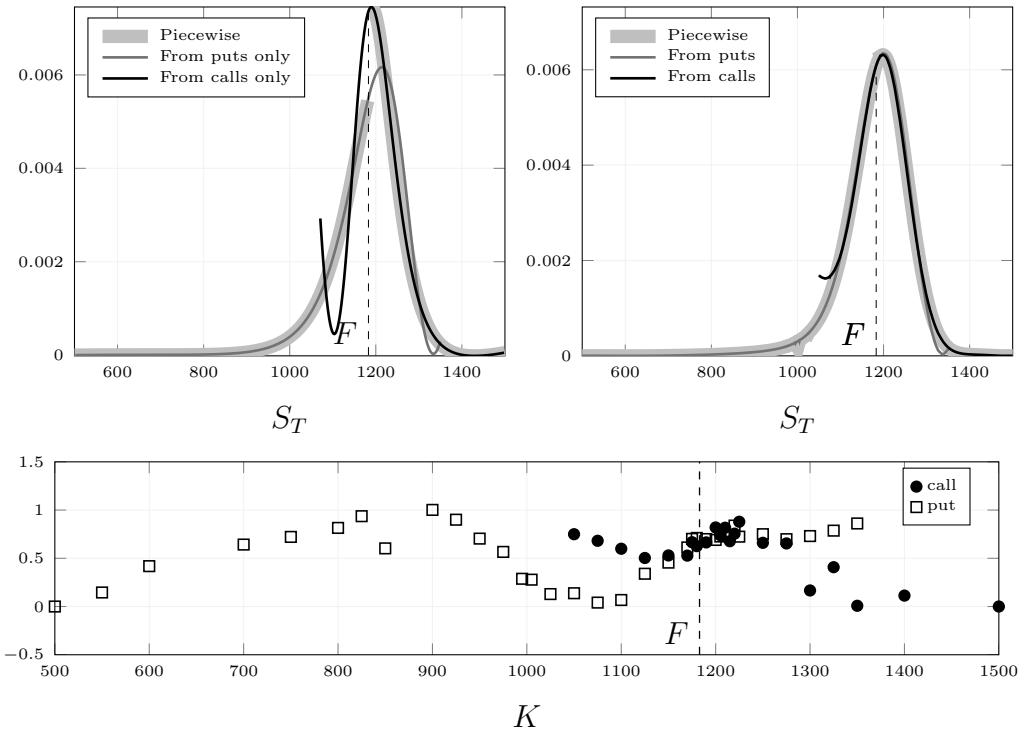

Figure 7: In the top panels, the thin gray line represent the implied RND derived from put option prices, the thin black line represent the one from call option prices, and the thick gray lines are the piecewise RNDs from the basic RII method for the left panel, and from the final improved RII method for the right panel. The bottom panel illustrates the relative positions of implied option prices, see expression (14). The vertical dashed line indicates the location of the forward price F.

value $F = S_0 e^{(r-\delta)T}$. Note that the forward value now includes the dividend yield. Since the rational approximations shown in Figure 6 already satisfy the (discretized) lower bound conditions (17), the previously presented results remain valid including no-arbitrage considerations. But we emphasize that the lower bounds of the bid-ask intervals should be intersected with the left-hand sides of (17). Also, recall from Appendix B that rational functions are determined with numerator degrees smaller than their denominator degrees, hence their values go asymptotically to zero in the respective regions where they are defined.

To illustrate the robustness of our RII method, we consider some additional S&P 500 index options. We arbitrarily choose the date of September

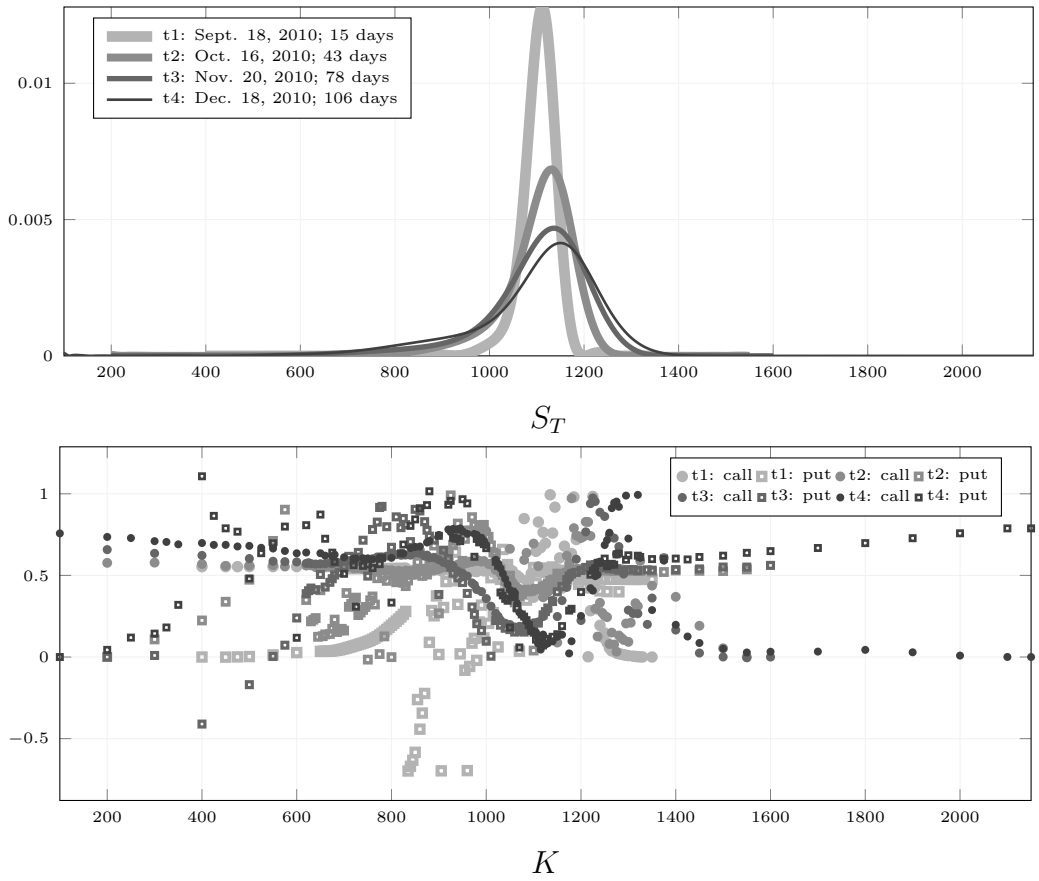

Figure 8: The top panel illustrates the single continuously differentiable implied RNDs derived from S&P 500 index option prices of September 3rd, 2010 with different maturity times by using our final improved RII method. The bottom panel represents their corresponding relative positions, defined in expression (14), for both European vanilla put option prices and call option prices with different maturity dates.

3rd, 2010, then extract the single continuously differentiable implied RNDs from the closing bid and ask prices with maturity times ranging from 2 weeks to around 3 months, that is, with the maturity dates on September 18th, 2010 (15 days), October 16th, 2010 (43 days), November 20th, 2010 (78 days) and December 18th, 2010 (106 days). The obtained implied RNDs as well as their corresponding relative positions for both implied European vanilla put option prices and call option prices are shown in Figure 8. The worst result is in the scenario with 15 days to maturity. The PDF of such

short maturity contracts are often badly behaved because of the price effects from trading strategies related to contract expiration and rollover of hedge positions into later expirations [44]. Even for this worst case, the relative positions are mostly within their bid and ask intervals, i.e. between $[0, 1]$ in Figure 8 (bottom). For other cases, the results are much better.

6. Conclusions

We find that for any setting, the RII method presented here is more robust to increasing noise levels on the option prices than both the DLN and IVS method. Moreover, in contrast to the DLN and IVS method, the RII method retains the ability to retrieve an acceptable RND in the more realistic test cases of the Heston and CGMY model. The RII method is also better suited for working with longer maturity options, a property that may be related to its ability to recover distributions with fat tails. The only region where significant discrepancies between the option implied RND and the test RND can be found is for option prices well in-the-money: this tail of the distribution can be overestimated when the absolute noise on the option price becomes large.

When applying the method to real market data, we rely on both European vanilla call and put options, combining the complementary out-of-the-money regions. We use the relative position of the result within the bid and ask interval as an indicator for the quality of the result.

The method and techniques outlined here allow to determine implied RNDs that are model-independent and do not suffer from time-dependent effects in historical data. As future work, this opens the way to study the role of the scale-free characteristics of these densities near critical points. In [49], it is shown that the (short-time) non-Gaussian nature of the detrended log returns of the S&P 500 shows a scale-invariant behavior when the black Monday crash is included in the time series used to reconstruct the distribution of log returns. They interpret this as the onset of critical phenomena usually linked to phase transtions in physical systems. In order to avoid using large time windows for time series [49], it can be useful to study this criticality by reconstructing the market expectation for the distribution of log returns from option price data rather than from time series. The formalism proposed in this paper suits this purpose while not making an a priori choice for the form of the overall distribution.

References

[1] F. Black, M. S. Scholes, The pricing of options and corporate liabilities, Journal of Political Economy 81 (3) (1973) 637–54.

[2] S. L. Heston, A closed-form solution for options with stochastic volatility with applications to bond and currency options, Review of Financial Studies 6 (2) (1993) 327–43.

[3] D. Duffie, J. Pan, K. Singleton, Transform analysis and asset pricing for affine jump-diffusions, Econometrica 68 (6) (2000) 1343–1376.

[4] L. Liang, D. Lemmens, J. Tempere, Generalized pricing formulas for stochastic volatility jump diffusion models applied to the exponential Vasicek model, The European Physical Journal B - Condensed Matter and Complex Systems 75 (2010) 335–342.

[5] W. Schoutens, Levy Processes in Finance: Pricing Financial Derivatives, 1st Edition, Wiley, New York, 2003.

[6] D. Lemmens, L. Liang, J. Tempere, A. D. Schepper, Pricing bounds for discrete arithmetic asian options under Lévy models, Physica A: Statistical Mechanics and its Applications 389 (22) (2010) 5193 – 5207.

[7] N. Cooper, Testing techniques for estimating implied RNDs from the prices of European-style options, in: Proceedings of the Bank for International Settlements Workshop on Estimating and Interpreting Probability Density Functions, Bank for International Settlements, Monetary and Economic Department, BIS, Basel, Switzerland, 1999.

[8] X. Liu, Bid-ask spread, strike prices and risk-neutral densities, Applied Financial Economics 17 (11) (2007) 887–900.

[9] P. W. Buchen, M. Kelly, The maximum entropy distribution of an asset inferred from option prices, Journal Of Financial And Quantitative Analysis 31 (1) (1996) 143–159.

[10] W. Guo, Maximum entropy in option pricing: A convex-spline smoothing method, Journal of Futures Markets 21 (9) (2001) 819–832.

[11] J. Borwein, R. Choksi, P. Maréchal, Probability distributions of assets inferred from option prices via the principle of maximum entropy, SIAM Journal on Optimization 14 (2) (2003) 464–478.

[12] J. O. Rodriguez, F. Santosa, Estimation of asset distributions from option prices: Analysis and regularization, SIAM Journal on Financial Mathematics 3 (1) (2012) 374–401.

[13] C. Bose, R. Murray, Maximum entropy estimates for risk-neutral probability measures with non-strictly-convex data, Journal of Optimization Theory and Applications 161 (1) (2014) 285–307.

[14] E. Jaynes, Information theory and statistical mechanics, Physical Review 106 (1957) 620–630.

[15] E. Jaynes, Information theory and statistical mechanics ii, Physical Review 108 (1957) 171–190.

[16] C. Neri, L. Schneider, Maximum entropy distributions inferred from option portfolios on an asset, Finance and Stochastics 16 (2) (2012) 293–318.

[17] E. Jondeau, M. Rockinger, Reading the smile: the message conveyed by methods which infer risk neutral densities, Journal of International Money and Finance 19 (6) (2000) 885 – 915.

[18] R. R. Bliss, N. Panigirtzoglou, Testing the stability of implied probability density functions, Journal of Banking & Finance 26 (2-3) (2002) 381–422.

[19] R. Cont, Beyond implied volatility: Extracting information from option prices, in: J. Kertesz, I. Kondor (Eds.), Econophysics: an emerging science, Kluwer, Dordrecht, Netherlands, 1998.

[20] J.-B. Monnier, Risk-neutral density recovery via spectral analysis, SIAM Journal on Financial Mathematics 4 (1) (2013) 650–667.

[21] J. M. Campa, P. H. K. Chang, R. L. Reider, W. H. Buiter, B. Eichengreen, ERM bandwidths for EMU and after: Evidence from foreign exchange options, Economic Policy 12 (24) (1997) 53–89.

[22] A. Bouden, Comparing risk neutral density estimation methods using simulated option data, in: S. I. Ao, L. Gelman, D. W. Hukins, A. Hunter, A. M. Korsunsky (Eds.), Proceedings of the World Congress on Engineering 2007 Vol I, WCE '07, July 2 - 4, 2007, London, U.K., Lecture Notes in Engineering and Computer Science, International Association of Engineers, Newswood Limited, 2007, pp. 1029–1037.

[23] J. C. Jackwerth, M. Rubinstein, Recovering probability distributions from option prices, The Journal of Finance 51 (5) (1996) 1611–1631.

[24] A. M. Monteiro, R. H. Tütüncü, L. N. Vicente, Recovering risk-neutral probability density functions from options prices using cubic splines and ensuring nonnegativity, European Journal of Operational Research 187 (2) (2008) 525 – 542.

[25] D. T. Breeden, R. H. Litzenberger, Prices of state-contingent claims implicit in option prices, The Journal of Business 51 (4) (1978) 621–651.

[26] A. M. Malz, Estimating the probability distribution of the future exchange rate from option prices, The Journal of Business 5 (2) (1997) 18–36.

[27] M. Fengler, Arbitrage-free smoothing of the implied volatility surface, Quantitative Finance 9 (04) (2009) 417–428.

[28] B. Brunner, R. Hafner, Arbitrage-free estimation of the risk-neutral density from the implied volatility smile, The Journal of Computational Finance 7 (1) (2003) 75–106.

[29] B. Bahra, Implied Risk-neutral Probability Density Functions From Option Prices: Theory and Application, Working Paper 66, Bank of England (1997).

[30] E. Glatzer, M. Scheicher, Modelling the Implied Probability of Stock Market Movements, in: ECB workshop on The Measures and Determinants of Financial Market Uncertainty, no. 212 in European Central Bank working paper series, Frankfurt am Main, Germany, 2003.

[31] M. Andersson, M. Lomakka, Evaluating implied RNDs by some new confidence interval estimation techniques, Journal of Banking and Finance 29 (6) (2005) 1535 – 1557.

[32] L. N. Trefethen, Approximation Theory and Approximation Practice, SIAM, 2013.

[33] P. Gonnet, R. Pachón, L. N. Trefethen, Robust rational interpolation and least-squares, Electronic Transactions on Numerical Analysis 38 (2011) 146–167.

[34] O. Salazar Celis, A. Cuyt, B. Verdonk, Rational approximation of vertical segments, Numerical Algorithms 45 (2007) 375–388.

[35] R. Pacanowski, O. Salazar Celis, C. Schlick, X. Granier, P. Poulin, A. Cuyt, Rational BRDF, IEEE Transactions on Visualization and Computer Graphics 18 (11) (2012) 1824–1835.

[36] T. Pomentale, On discrete rational least squares approximation, Numerische Mathematik 12 (1) (1968) 40–46.

[37] H. T. Nguyen, A. Cuyt, O. Salazar Celis, Comonotone and coconvex rational interpolation and approximation, Numerical Algorithms 58 (1) (2011) 1–21.

[38] P. Carr, H. Geman, D. B. Madan, M. Yor, The fine structure of asset returns: An empirical investigation, The Journal of Business 75 (2) (2002) 305–332.

[39] R. Cont, P. Tankov, Financial modelling with jump processes, Chapman & Hall / CRC, 2004.

[40] H. Kleinert, Path Integrals in Quantum Mechanics, Statistics, Polymer Physics, and Financial Markets, 5th Edition, World Scientific Publishing Company, Singapore, 2009.

[41] S. N. Neftci, Principles of Financial Engineering, 2nd Edition, Academic Press, 2008.

[42] K. Back, A Course in Derivative Securities: Introduction to Theory and Computation, Springer, 2010.

[43] D. Stefanica, A Primer For The Mathematics Of Financial Engineering, FE Press, 2011.

[44] S. Figlewski, Volatility and Time Series Econometrics: Essays in Honor of Robert Engle, Oxford University Press, 2008, Ch. Estimating the Implied Risk Neutral Density for the U.S. Market Portfolio.

[45] I. Barrodale, F. D. K. Roberts, An improved algorithm for discrete l_1 linear approximation, SIAM Journal on Numerical Analysis 10 (5) (1973) 839–848.

[46] S. Boyd, L. Vandenberghe, Convex optimization, Cambridge University Press, 2004.

[47] The CBOE Volatility Index - VIX, White paper, Chicago Board Options Exchange (2009).

[48] M. Roper, Arbitrage free implied volatility surfaces, Preprint, School of Mathematics and Statistics, The University of Sydney (March 2010).
URL `http://www.maths.usyd.edu.au/u/pubs/publist/preprints/2010/roper-9.pdf`

[49] K. Kiyono, Z. R. Struzik, Y. Yamamoto, Criticality and phase transition in stock-price fluctuations, Physical review letters 96 (6) (2006) 068701.

Appendix A. Benchmark details

Table A.2 summarizes the parameters of each of the three market models used in the benchmark. Table A.3 summarizes the skewness and kurtosis values of the associated distributions. Table A.4 summarizes the normalized errors of the different methods to derive the implied RNDs.

Table A.2: Summary of the parameters and their chosen values for the three market models used in the benchmark.

Black Scholes	Heston	CGMY
$S_0 = 925$, $r = 0.03$	$S_0 = 925$, $r = 0.03$	$S_0 = 925$, $r = 0.03$
$\mu = 0.05$, $\sigma = 0.2$	$\mu = 0.05$, $\sigma_v = 0.1$	$C = 0.0244$, $G = 0.0765$
	$\kappa = 2$, $\theta = 0.04$	$M = 7.5515$, $Y = 1.2945$
	$\rho = 0.5$, $v_0 = 0.0437$	

Table A.3: Summary of skewness and kurtosis values for each of the distributions and different times to maturity T.

T	Black-Scholes		Heston		CGMY	
	Skewness	Kurtosis	Skewness	Kurtosis	Skewness	Kurtosis
0.0384	0.0998	1.3833	0.0544	1.3834	1.6037	4.1906
0.5	0.1361	1.3970	0.1524	1.4151	0.8156	2.1193
1.5	0.2139	1.4365	0.2732	1.4839	0.4892	1.6625

Table A.4: Summary of the normalized errors of the different methods to derive the implied RNDs. The results are presented for different times to maturity T and values of the noise control parameter η.

η	T	Black-Scholes			Heston			CGMY		
		DLN	IVS	RII	DLN	IVS	RII	DLN	IVS	RII
1	0.038	0.0052	0.0060	0.0009	0.0056	0.0095	0.0009	0.054	0.0066	0.0026
	0.5	0.455	0.010	0.0011	0.069	0.038	0.0013	0.13	0.0139	0.0029
	1.5	0.429	0.012	0.0006	0.064	0.047	0.0008	0.15	3.4153	0.0017
10	0.038	0.003	0.069	0.0061	0.029	0.069	0.0055	0.056	0.0338	0.0080
	0.5	0.455	0.099	0.0021	0.070	0.31	0.0028	0.13	0.0907	0.0078
	1.5	0.0009	0.096	0.0022	0.067	0.496	0.0025	0.104	3.4584	0.0057
100	0.038	0.006	6.5	0.0072	0.030	5.3	0.0068	0.055	1.0549	0.0099
	0.5	0.030	1.40	0.0147	0.060	2.7	0.0137	0.075	3.1959	0.0156
	1.5	0.432	0.92	0.0140	0.288	7.1	0.0119	0.36	0.6260	0.0145

Appendix B. The simultaneous call-put RII method

Of the same underlying, we assume to be given n_1+1 call intervals $[\underline{c}_i, \overline{c}_i]$ at strike locations K_i^{call} $(i = 0, \ldots, n_1)$ and n_2+1 put intervals $[\underline{p}_i, \overline{p}_i]$ at strike locations K_i^{put} $(i = 0, \ldots, n_2)$. Denote the common call-put denominator polynomial of degree m by

$$q_m(K) = \sum_{i=0}^{m} \beta_i K^i.$$

We are looking for two rational functions

$$r_{\ell_1,m}^{\text{call}}(K) = \frac{p_{\ell_1}^{\text{call}}(K)}{q_m(K)} \quad \text{and} \quad r_{\ell_2,m}^{\text{put}}(K) = \frac{p_{\ell_2}^{\text{put}}(K)}{q_m(K)},$$

with respective numerator polynomials

$$p_{\ell_1}^{\text{call}}(K) = \sum_{i=0}^{\ell_1} \alpha_i^{(1)} K^i, \qquad p_{\ell_2}^{\text{put}}(K) = \sum_{i=0}^{\ell_2} \alpha_i^{(2)} K^i,$$

for which the following conditions are satisfied:

$$\begin{cases} \underline{c}_i \le r_{\ell_1,m}^{\text{call}}(K_i^{\text{call}}) \le \overline{c}_i, & i = 0, \ldots, n_1, \\ \underline{p}_i \le r_{\ell_2,m}^{\text{put}}(K_i^{\text{put}}) \le \overline{p}_i, & i = 0, \ldots, n_2, \\ -e^{-rT} \le r_{\ell_1,m}^{\prime\,\text{call}}(K_i^{\text{call}}) \le 0, & i = 0, \ldots, n_1, \\ 0 \le r_{\ell_2,m}^{\prime\,\text{put}}(K_i^{\text{put}}) \le e^{-rT}, & i = 0, \ldots, n_2, \\ 0 \le r_{\ell_1,m}^{\prime\prime\,\text{call}}(K_i^{\text{call}}), & i = 0, \ldots, n_1, \\ 0 \le r_{\ell_2,m}^{\prime\prime\,\text{put}}(K_i^{\text{put}}), & i = 0, \ldots, n_2. \end{cases} \tag{B.1}$$

Denote the vector of combined coefficients by

$$\mathbf{c} = (\alpha_0^{(1)}, \ldots, \alpha_{\ell_1}^{(1)}, \alpha_0^{(2)}, \ldots, \alpha_{\ell_2}^{(2)}, \beta_0, \ldots, \beta_m)^T \in \mathbb{R}^{\ell_1+\ell_2+m+3}$$

and denote by $\mathbf{A}$ the $(10n_1+10n_2+20) \times (\ell_1+\ell_2+m+3)$ constraint matrix composed of the linear inequalities ensuring (B.1). Note that this matrix has many zero entries. A nontrivial vector $\mathbf{c} \neq \mathbf{0}$ which strictly satisfies the component wise inequalities $\mathbf{Ac} \le 0$, can then be obtained in a similar way

as before. Hence by solving the strictly convex quadratic programming (QP) problem:

$$\begin{aligned} & \arg \min_{\mathbf{c}\in\mathbb{R}^{\ell_1+\ell_2+m+3}} \left(\|\mathbf{c}\|_2\right)^2 \\ \text{subject to} \quad & \mathbf{A}_j\mathbf{c} \le -\varepsilon \left\|\mathbf{A}_j\right\|_2, \quad j = 1, \ldots, 10n_1 + 10n_2 + 20. \end{aligned}$$

Here $\varepsilon > 0$ is an arbitrary positive constant, $\mathbf{A}_j$ denotes the j-th row of the matrix $\mathbf{A}$ and $\|\cdot\|_2$ is the Euclidean norm.

When $r^{\text{call}}_{\ell_1,m}(K)$ and $r^{\text{put}}_{\ell_2,m}(K)$ are only evaluated when they are out-of-the-money, as detailed in Appendix C, a natural choice for ℓ_1 and ℓ_2 is $\ell_1 = \ell_2 < m + 1$: like their associated option prices, such rational functions go asymptotically to zero.

Appendix C. Ensuring continuously differentiability

At the location of the forward value F, we add to the simultaneous call-put RII method that the piecewise implied density derived from $r^{\text{call}}_{\ell_1,m}(K) = p^{\text{call}}_{\ell_1}(K)/q_m(K)$ and $r^{\text{put}}_{\ell_2,m}(K) = p^{\text{put}}_{\ell_2}(K)/q_m(K)$ is continuously differentiable at $K = F$. So we require

$$\begin{cases} r''^{\,\text{call}}_{\ell_1,m}(F) = r''^{\,\text{put}}_{\ell_2,m}(F), \\ r'''^{\,\text{call}}_{\ell_1,m}(F) = r'''^{\,\text{put}}_{\ell_2,m}(F). \end{cases} \tag{C.1}$$

Without any further consideration, these conditions are essentially nonlinear equations in the unknown coefficients. However, we show how (C.1) can be guaranteed by the following linear conditions. Basically, the rational approximations $r^{\text{call}}_{\ell_1,m}(K)$ and $r^{\text{put}}_{\ell_2,m}(K)$ need to share some additional theoretical relations that exist between $C(S_0, K, T)$ and $P(S_0, K, T)$ at $K = F$.

First, it is known that *at-the-money* (hence when $K = F$) is the only status where the price of a call option and a put option are the same. Therefore we impose that

$$r^{\text{call}}_{\ell_1,m}(F) = r^{\text{put}}_{\ell_2,m}(F). \tag{C.2}$$

Provided that $q_m(F) \neq 0$, one readily obtains that (C.2) implies

$$p^{\text{call}}_{\ell_1}(F) - p^{\text{put}}_{\ell_2}(F) = 0. \tag{C.3}$$

Without loss of generality, we put $q_m(F) > 0$. At this point it is worth emphasizing that, when $\underline{c}_i < \overline{c}_i$ and if the linear inequalities (7) are strictly

satisfied, then it follows that $q_m(K_i^{\text{call}}) > 0$. A similar reasoning holds of course for $q_m(K_i^{\text{put}})$. As a consequence, the denominator $q_m(K)$ obtained from solving the proposed QP problem(s) always satisfies $q_m(K_i^{\text{call}}) > 0$ and $q_m(K_i^{\text{put}}) > 0$ by construction. Because the forward value F may not belong to either the given K_i^{call} or the given K_i^{put}, a nonzero condition such as $q_m(F) > 0$ needs to be added for (C.3) to imply (C.2).

Second, from the put–call parity (16) follows

$$\frac{\partial P(S_0, K, T)}{\partial K} = e^{-rT} + \frac{\partial C(S_0, K, T)}{\partial K}.$$

Therefore we also impose that

$$r'^{\,\text{put}}_{\ell_1,m}(F) = e^{-rT} + r'^{\,\text{call}}_{\ell_2,m}(F). \tag{C.4}$$

Given that $q_m(F) > 0$ and $r^{\text{call}}_{\ell_1,m}(F) = r^{\text{put}}_{\ell_2,m}(F)$, (C.4) is satisfied if and only if

$$p'^{\,\text{put}}_{\ell_2}(F) - p'^{\,\text{call}}_{\ell_1}(F) - e^{-rT} q_m(F) = 0. \tag{C.5}$$

Combining all the above, it is not difficult to find that (C.1) is satisfied if the linear inequality $q_m(F) > 0$, the linear equalities (C.3), (C.5) and

$$p''^{\,\text{put}}_{\ell_2}(F) - p''^{\,\text{call}}_{\ell_1}(F) - 2e^{-rT} q'_m(F) = 0, \tag{C.6}$$

$$p'''^{\,\text{put}}_{\ell_2}(F) - p'''^{\,\text{call}}_{\ell_1}(F) - 3e^{-rT} q''_m(F) = 0, \tag{C.7}$$

are satisfied. The converse is also true after (re)normalizing such that $q_m(F) > 0$. Following a similar reasoning, even higher orders of smoothness can be imposed if desired.